tvst

Article

Long-Term Decrease of Intraocular Pressure in Rats by Viral Delivery of miR-146a

Coralia Luna[1], Megan Parker[1], Pratap Challa[1], and Pedro Gonzalez[1]

[1] Duke University Eye Center, Durham, NC, USA

Correspondence: Pedro Gonzalez, Duke University Eye Center, Erwin Road, Box 3802, Durham, NC 27710, USA. e-mail: pedro.gonzalez@duke.edu

Received: January 21, 2021
Accepted: April 22, 2021
Published: July 13, 2021

Keywords: glaucoma; gene therapy; molecular biology

Citation: Luna C, Parker M, Challa P, Gonzalez P. Long-term decrease of intraocular pressure in rats by viral delivery of miR-146a. Transl Vis Sci Technol. 2021;10(8):14, https://doi.org/10.1167/tvst.10.8.14

Purpose: To evaluate the effects of miR-146a in trabecular meshwork (TM) cells and on intraocular pressure (IOP) in vivo via viral delivery of miR-146a to the anterior chamber of rat eyes.

Methods: Human TM cells were transfected with miR-146 mimic or inhibitor. Some cells from each group were then subjected to cyclic mechanical stress (CMS). Other cells from each group had no force applied. Gene expression was then analyzed by quantitative polymerase chain reaction (qPCR). Replication-deficient adenovirus and lentivirus expressing miR-146a were inoculated into the anterior segment of Brown Norway rat eyes. IOP was monitored by rebound tonometry, visual acuity was evaluated by optokinetic tracking (OKT), and inflammation markers in the anterior segment were examined by slit-lamp, qPCR, and semi-thin sections.

Results: miR-146 affected the expression of genes potentially involved in outflow homeostasis at basal levels and under CMS. Both lentiviral and adenoviral vectors expressing miR-146a resulted in sustained decreases in IOP ranging from 2.6 to 4.4 mmHg. Long term follow-up of rats injected with lentiviral vectors showed a sustained effect on IOP of 4.4 $\pm$ 2.9 mmHg that lasted until rats were sacrificed more than 8 months later. Eyes showed no signs of inflammation, loss of visual acuity, or other visible abnormalities.

Conclusions: Intracameral delivery of miR-146a can provide a long-term decrease of IOP in rats without signs of inflammation or other visible adverse effects.

Transitional Relevance: The IOP-lowering effects of miR-146 observed in rats provides a necessary step toward the development of an effective gene therapy for glaucoma in humans.

Introduction

Primary open angle glaucoma is the most prevalent type of glaucoma in the United States. It affects about 2% of individuals over age 40, accounting for 6% of all blindness and 19% of blindness among African Americans.[1] Gene therapy is an attractive approach for diseases of the eye because of the easy accessibility, low doses required for vector delivery, and relative immune privilege.[2] Gene therapy has been successfully applied to monogenic disorders of the eye but not so successfully to complex disorders, although there have been clinical trials for macular degeneration, macular edema, and glaucoma.[2] A small interfering RNA against a β2-adrenergic receptor (ADRB2) has been shown to reduce intraocular pressure (IOP) in humans in phase I and II of clinical trials (Gonzalez V. *IOVS*. 2014;55:ARVO E-Abstract 564).[3] However, although important efforts have been made to develop a gene therapy to treat ocular hypertension, an effective therapy for lowering IOP for long periods of time (at least 6 months) with low cytotoxicity or other adverse effects is not currently available. Attempts to develop a gene therapy for ocular hypertension have encountered significant problems, such as low effects on IOP, presence of adverse effects, and short duration of IOP-lowering effects.[4–21] Therefore, the identification of new effective targets is essential to developing a gene therapy for ocular hypertension.

MicroRNAs (miRNAs) are attractive tools to achieve prolonged modulation of biological functions,

such as IOP, because of their stability and capacity to regulate entire networks of genes to achieve specific functional effects.[22] Their use in gene therapy has some advantages due to their small size compared with larger genes, which allows them to be carried by many different vectors. In addition, miRNAs show relatively low cytotoxicity compared with DNA gene or protein therapies.[23]

miR-146a (miRBase: MI0000477; symbol, MIR146A; HGNC ID, HGNC:31533) has been shown to play a critical role in fibrosis and the inflammatory response.[24–28] In the past, we found that miR-146a was upregulated in senescent fibroblasts and trabecular meshwork (TM) cells and that its upregulation could act as a brake to excessive production of inflammatory cytokines that are part of the senescence-associated secretory phenotype.[29] Additional studies have shown that miR-146a is upregulated by cyclic mechanical stress (CMS) in TM cells.[30] The TM is constantly subject to mechanical forces such as IOP spikes, cardiac cycle, blinking, and eye movement. These changes in IOP result in cyclic stretching of TM cells, and it has been hypothesized that cellular responses to such stretching may play a significant role in both homeostasis and pathological alterations of the outflow.[31–37] The aim of this study was to investigate the potential role of miR-146a in intraocular pressure modulation and evaluate its potential as a gene therapy target for ocular hypertension.

Materials and Methods

Cell Culture, miRNA Transfection, and Virus Transduction

Human trabecular meshwork (HTM) primary cell cultures were generated from cadaver eyes or cornea rings from donors with no history of eye disease and were validated as previously reported.[38] Cell cultures were maintained at 37°C in 5% CO_2 in media (low-glucose Dulbecco's Modified Eagle Medium [DMEM] with L-glutamine, 110 mg/mL sodium pyruvate, 10% fetal bovine serum, 100 mM non-essential amino acids, and 100 units/mL penicillin). All reagents were obtained from Thermo Fisher Scientific (Waltham, MA). HTM primary cells, passage 3 to 4 (HTM L3, from a 25-year-old donor, HTM 1788, from a 23-year-old donor) were transfected at around 70% confluency 1 day after plating using Lipofectamine 2000 (Thermo Fisher Scientific) and following the manufacturer's instructions. Cells were transfected with hsa-miR-146a mimic (146M), hsa-miR-146a inhibitor (146I), and their respective negative controls, scrambled mimic or scrambled inhibitor, at 40-pM concentration (Dharmacon, Chicago, IL) and analyzed 72 hours after transfection. HTM cells transduced with adenovirus (Ad-CAG-miR-146a or Ad-CAG-empty, 50 plaque-forming units [pfu] each) were analyzed 72 hours after transduction. HTM cells transduced with lentivirus (Lenti-CAG-miR-146a, 30 pfu) were analyzed 1 week after transduction.

Cyclic Mechanical Stress

HTM cell cultures were plated on type I collagen-coated flexible silicone bottom plates (Flexcell International, Hillsborough, NC) and transfected 24 hours later with miRNAs. Cells were subjected to CMS 72 hours after transfection. The medium was switched to serum-free DMEM 2 hours before CMS. The cells were stretched for 4 hours (20% stretching, one cycle per second) using the computer-controlled and vacuum-operated Flexercell Strain Unit FX-3000 (Flexcell International). A frequency of one cycle per second was selected to mimic cardiac frequency. Control cells were cultured under the same conditions, but no mechanical force was applied.

Quantitative Polymerase Chain Reaction

Total RNA was isolated from HTM cells and from the anterior chambers of rat eyes (cornea, trabecular meshwork, ciliary body, and a small fraction of iris and sclera) using the Direct-zol RNA MiniPrep Kit (Zymo Research, Irvine, CA) according to manufacturer's instructions. RNA yields were measured using a NanoDrop spectrophotometer (Thermo Fisher Scientific). First-strand complementary DNA (cDNA) was synthesized from total RNA (700 ng cells and 500 ng tissue) by reverse transcription using oligo(dT) and SuperScript II Reverse Transcriptase (Invitrogen, Carlsbad, CA) according to the manufacturer's instructions. Quantitative polymerase chain reaction (qPCR) was performed using 20-µL mixtures containing 1 µL of the cDNA preparation and 1× iQ SYBR Green Supermix (Bio-Rad, Hercules, CA). The following PCR parameters were used: 95°C for 3 minutes followed by 40 cycles at 95°C for 15 seconds, 55°C for 15 seconds, and 72°C for 15 seconds. Beta actin and glyceraldehyde-3P-dehydrogenase (GAPDH) were used as an internal normalized reference for cDNA. miRNA cDNA (50 ng) was transcribed using the TaqMan MicroRNA Reverse Transcription Kit and TaqMan MicroRNA assays for miR-146a and RNU6B (normalized reference; Thermo Fisher Scientific). It was then amplified using the TaqMan Universal PCR Master Mix, following the manufacturer's instructions.

Table. Primers Used for qPCR

Name	NCBI Gene ID	Forward 5′–3′	Reverse 5′–3′
Hs.COX1	5742	TAGAGATTGGGGCTCCCTTT	AGGGACAGGTCTTGGTGTTG
Hs.COX2	5743	TGAGCATCTACGGTTTGCTG	TGCTTGTCTGGAACAACTGC
Hs.IL1β	3553	AACAGGCTGCTCTGGGATTCTCTT	ATTTCACTGGCGAGCTCAGGTACT
Hs.IL8	3576	AGAAACCACCGGAAGGAACCATCT	CACCTTCACACAGAGCTGCAGAAA
Hs.IL6	3569	AAATTCGGTACATCCTCGACGG	AGTGCCTCTTTGCTGCTTTCACAC
Hs.PAI1	5054	AATGTGTCATTTCCGGCTGCTGTG	ACATCCATCTTTGTGCCCTACCCT
Hs.IRAK1	3654	ATTTATGCTTGGGAGGTCGAGGC	TCGCTTCTTGCTAGGACTGAACCA
Hs.HSP70	3310	ACAGGAGCACAGGTAAGGCT	TTCATGAACCATCCTCTCCA
Hs.GADPH	2597	TCAACAGCGACACCCACTCCT C	ATGAGGTCCACCACCCTGTTGC
Hs.beta actin	60	CCTCGCCTTTGCCGATCCG	GCCGGAGCCGTTGTCGACG
Rn.TNFα	24835	GGTCCCAACAAGGAGGAGAA	GCTTGGTGGTTTGCTACGAC
Rn.IL1β	24494	CACTCATTGTGGCTGTGGAG	AGGACGGGCTCTTCTTCAAA
Rn.CD68	287435	ACGGACAGCTTACCTTTGGA	AATGTCCACTGTGCTGCTTG
Rn.GADPH	24383	AAGATGGTGAAGGTCGGTGT	GCTTCCCATTCTCAGCCTTG
Rn.beta actin	81822	TCCTCCCTGGAGAAGAGCTA	ACGGATGTCAACGTCACACT

The absence of nonspecific products was confirmed by melting curve analysis. All qPCR experiments were performed with a CFX96 thermal cycler (Bio-Rad). Results from qPCR are expressed as $2^{-\Delta Ct}$ (delta CT) and are represented as a percentage of the control ± SD or as $2^{-\Delta\Delta Ct}$ (fold) ± SD. The primers used for qPCR amplification were designed using Primer 3[39] and are shown in the Table.

Recombinant Adenovirus, Lentivirus, and Adeno-Associated Virus Preparation

To prepare adenovirus expressing miR-146a under the CAG promoter system (Ad-CAG-miR-146a) or a control "empty" adenovirus (Ad-CAG-empty), pENTR1A (Thermo Fisher Scientific) was modified to eliminate the restriction sites for Not1 and EcoR1 from the multiple cloning site by PCR amplification using the following primers: F, 5′-AAAAGCTTGCCGCACTCGAGATATCTAGACC3′; R, 5′-CGGTACCGGATCCA**GTCGAC**TGAATTG-GTTC3′ (restriction sites are in bold). This was followed by digestion of the PCR product with SalI and HindIII and ligation to the fragment generated from the digestion of the pCAGEN plasmid (11160; Addgene, Watertown, MA) with SalI and HindIII. The fragment from pCAGEN contains the CAG promoter, a multiple cloning site (EcoRi/XhoI/EcorV/NotI), and rabbit globin polyA signal.[40] miR-146a was obtained through PCR amplification of the pre-miRNA region from plasmid 15092 (Addgene)[41] using the following primers: F, 5′-T**GGTCTC**TAATTGGCTGGGACAGGCCTGGAC-3′; R, 5′AG**GCGGCCGC**TCGAGGAGCCTGAGA CTCTG-3′ (restriction sites are in bold; BsaI with EcoRI end and NotI). miR-146a PCR product was cloned into pENTR1A-CAG and digested with EcoRI and NotI to generate pENTR-CAG-146a; miR-146a was confirmed by sequencing. Recombinant adenoviruses for miR-146a and empty plasmid (pENTR1A-CAG) were prepared using the Invitrogen Gateway system, following the manufacturer's instructions. CAG-mir-146a/pENTR1A or CAG-/pENTR1A were recombined with pAd/PL-DEST (Invitrogen) using LR recombinase (Invitrogen). miR-146a was resequenced for confirmation. Adenoviruses were amplified, purified, and titer determined using the Adenovirus Mini Purification Kit (Virapur, San Diego, CA) and the Adeno-X Rapid Titer Kit (Clontech, Mountain View, CA), following the manufacturer's instructions.

For adeno-associated virus (AAV) preparation, the PCR fragment of miR-146 was digested with BsaI (with compatible EcoRI end) and NotI, and cloned between the BamHI and NotI sites of pscAAV-CAG-GFP plasmid (83279; Addgene),[42] which resulted in replacement of the *GFP* gene with miR-146a to generate the pscAAV-CAG-miR-146a plasmid. To generate lentivirus-expressing miR-146a under the CAG promoter, the IRES-GFP fragment from vector plenti-CAG-IRES-GFP (69047; Addgene)[43] was replaced with miR-146a by digestion of plenti-CAG-IRES-GFP with EcoRI and NotI and miR-146 with BsaI with EcoRI compatible end and NotI.

Both lentivirus and AAVs were prepared at the Duke University School of Medicine Viral Vector Core. The lentivirus vector is based on the human immunodeficiency virus (HIV) pseudotyped with the vesicular stomatitis virus G-protein. AAV viruses (miR-146 and GFP) are self-complementary AAV (scAAV) type 2 vectors with miR-146a and GFP driven by the same CAG promoter.

In Vivo Injections, IOP Measurements, and Ophthalmologic Examinations

All experiments with animals were conducted in accordance with the ARVO Statement for the Use of Animals in Ophthalmic and Vision Research and were approved by the Institutional Animal Care and Use Committee at Duke University. Retired Brown Norway female breeder rats (age, 8–12 months) from Charles River Laboratories (Wilmington, MA), were housed in pairs with a 12-hour cycle of light and dark; the average luminosity during the light cycle was 184.25 ± 22.5 lux ($n = 4$) 1 m above the floor and was 11.25 ± 7.67 lux ($n = 4$) inside the cages. The rats received water and food ad libitum. For intraocular injections, rats were anesthetized with a mixture of oxygen and isofluorane (V-1 Tabletop Laboratory Animal Anesthesia System; VetEquip, Pleasanton, CA) plus a drop of topical anesthetic (proparacaine hydrochloride; Akorn Pharmaceuticals, Lake Forest, IL). Rats were injected with viral suspension in one eye using insulin syringes with an ultra-fine needle (31-gauge; BD Biosciences, San Jose, CA), and the contralateral eye was used as a control. Injections were conducted for all vectors in the right eye regardless of the basal IOPs to prevent any potential bias in the choice of eye injected. The needle was inserted through the peripheral cornea with the bevel up, and the bevel rotated 90° for viral inoculation. Ten rats were injected with adenovirus Ad-CAG-miR-146a and six rats with adenovirus Ad-CAG-empty (both with 1.5×10^{11} pfu/mL, 15 µL); 10 rats were injected with AAV-CAG-miR-146a and six rats with AAV-CAG-GFP (both with 3×10^{13} pfu/mL, 15 µL); and nine rats were injected with Lenti-CAG-miR-146a (three rats with 5.6×10^{8}, 25µL, and six rats with 1.0×10^{9} pfu/mL, 15 µL).

IOP was measured in awake animals using topical anesthetic two times a week for the first 3 months and once a week after that. Measurements were taken at the same time of the day (between 8:30 AM and 10:00 AM) with an average of six readings per eye using a portable tonometer (TonoLab; iCare, Vantaa, Finland). The measurements of IOPs were conducted in a masked manner (by a person not involved in the injections) for the adenoviral vectors and for the first 3 months of the lentiviral vectors. After that point, IOPs had to be measured by the same personnel who conducted the injections. Examinations of the anterior chamber structures (corneal epithelium, endothelium, chamber depth, lens status, and inflammation) were performed in a masked manner by a board-certified ophthalmologist (P.C.) using a slit-lamp biomicroscope (SL-2E Slit Lamp; Topcon, Tokyo, Japan) and an ophthalmoscope (Universal S3; Carl Zeiss, Oberkochen, Germany).

Optomotor Response

Visual function was evaluated by optokinetic tracking (OKT) using OptoMotry (CerebralMechanics, Medicine Hat, Alberta, Canada).[44] Briefly, rats were placed on an elevated platform in the middle of a chamber surrounded by screen monitors displaying vertical gratings rotating at a speed of 12°/s. A camera situated above imaged the behavior of the animal, and a cursor was placed on the forehead of the animal to allow the observer to track the head movement. The movement was tracked clockwise (left eye) or counterclockwise (right eye) in response to the rotating gratings in real time. To determine the spatial frequency threshold, the vertical bands were displayed at 100% contrast starting at 0.042 cycles/deg, and the spatial frequency was increased until the animal no longer tracked.

Semi-Thin Sections

Control (not injected) and experimental (injected with Lenti-CAG-miR-146a) eyes were enucleated, washed in phosphate-buffered saline (PBS), and fixed in 2% glutaraldehyde/2% paraformaldehyde in PBS. Post-fixation, they were placed in 1% osmium tetroxide, dehydrated, embedded in epoxy, sectioned (0.5 µm), and stained at the Morphology Facility at Duke University Eye Center. Semi-thin sections were examined by light microscopy (Axioplan 2; Carl Zeiss).

Statistical Analyses

Paired Student's t-test was used for IOP comparison among Lenti-CAG-miR-146a, Ad-CAG-miR-146a, and Ad-CAG-empty and their respective contralateral control (non-injected) eyes. Data are presented as mean ± SD. Results from qPCR are represented as a percentage of the control ± SD or fold ± SD. Significance for qPCR was evaluated using the unpaired Student's t-test. $P < 0.05$ was considered significant.

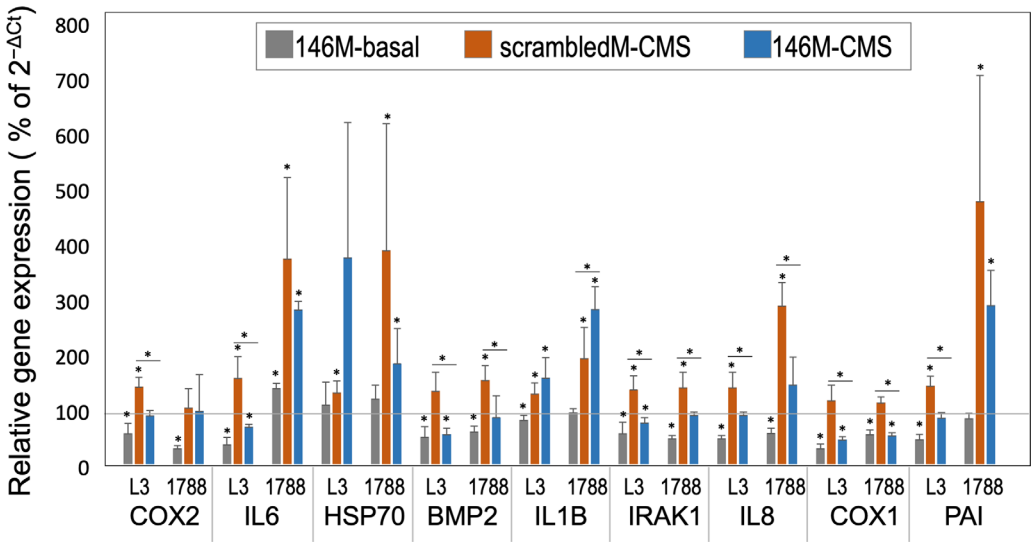

Figure 1. Effects of overexpression of miR-146a on gene expression in HTM cells at the basal level and under CMS. Gene expression of two primary HTM cells (L3 and 1788) was analyzed after transfection with miR-146a mimic or scrambled mimic under two experimental conditions: basal level or CMS. Gene expression in cells transfected with (1) miR-146a at the basal level (146M-basal), (2) miR-146a under CMS (146M-CMS), and (3) scrambled mimic under CMS (scrambledM-CMS) are represented as a percentage of expression in control cells transfected with scrambled mimic at basal conditions (horizontal line at 100). Each experiment was run in triplicate. The bars represent mean ± SD. The statistical significance was calculated using an unpaired *t*-test; $^{*}P < 0.05$ and $^{**}P < 0.01$.

Results

Effects of miR-146a Overexpression on HTM Cells Subjected to CMS

To follow up on the studies showing that miR-146 was upregulated by cyclic mechanical stress in HTM cells[30] and that its overexpression in HTM cells downregulated genes that could potentially affect outflow homeostasis,[29] two HTM primary cells lines were transduced with miR-146a mimic, miR-146 inhibitor, and their respective negative controls, scrambled mimic and scrambled inhibitor, and then were subjected to CMS or kept in the same conditions with no CMS. Nine genes were analyzed by qPCR (*COX2*, *IL6*, *HSP70*, *IRAK1*, *BMP2*, *PAI1*, *COX1*, *IL8*, and *IL1B*). Those genes were chosen because they were up- or downregulated by CMS and/or miR146 in previous experiments.

Under basal conditions (no CMS), HTM cells transfected with the miR-146 mimic showed significant downregulation for most of the genes analyzed, with an average of 34% decrease in gene expression compared with control cells transfected with a scrambled mimic, as shown in Figure 1. In addition, when cells were subjected to CMS, the induction of gene expression due to the stretching was also partially or totally inhibited in miR-146a–transduced cells for most of the analyzed genes. The average increase in expression of the selected genes was 93% for controls and 42% in cells treated with 146a mimic (Fig. 1).

To study the effects of miR-146a inhibition on gene expression, HTM cells were transfected with miR-146 inhibitor or scrambled inhibitor. Consistent with the effects observed after miR-146a overexpression, inhibition of miR-146a increased the basal expression levels of the analyzed genes an average of 106% compared with cells transfected with scrambled inhibitor. When subjected to CMS, cells transfected with miR-146 inhibitor showed an average increase in expression of the selected genes of 446% compared with cells transfected with scrambled inhibitor. However, this increase was not as homogeneously distributed among genes as the decrease in expression observed in cell transfected with 146a mimic for reasons that at this point we do not fully understand (Fig. 2).

Effect of Viral Delivery of miR-146a on IOP in Living Rat Eyes

Intracameral adenoviral injections of Ad-CAG-miR-146a in normotensive rat eyes resulted in a sustained decrease in IOP (average difference for contralateral eyes, 4.02 mmHg ± 1.99; $n = 10$), which lasted at least for 2 months (Fig. 3A). To ensure that the effect on IOP was specific to miR-146a, we injected

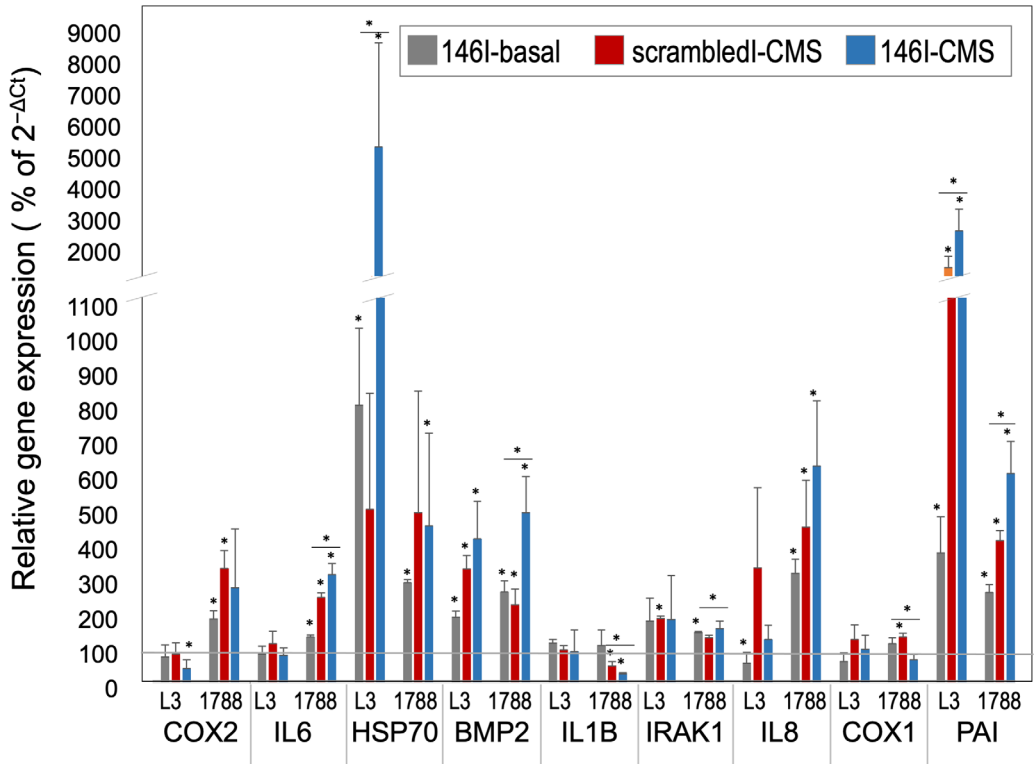

Figure 2. Effects of inhibition of miR-146a on HTM cells at the basal level and under CMS. Gene expression of two primary HTM cells (L3 and 1788) was analyzed after transfection with miR-146 inhibitor or scrambled inhibitor under two experimental conditions: basal level or CMS. Gene expression in cells transfected with (1) miR-146 inhibitor at basal level (146I-basal), (2) miR-146 inhibitor under CMS (146I-CMS), and (3) scrambled inhibitor under CMS (scrambledM-CMS) is represented as a percentage of expression in control cells transfected with scrambled inhibitor at basal conditions (horizontal line at 100). Each experiment was run in triplicate. The bars represent mean ± SD. The statistical significance was calculated using an unpaired *t*-test; $^{*}P < 0.05$ and $^{**}P < 0.01$.

a control virus with the same CAG promoter system but no insert. As shown in Figure 3B, no significant change in IOP was observed between injected and non-injected contralateral control eyes (average difference of 0.35 mmHg ± 0.84; $n = 6$). The ability of Ad-CAG-miR-146a to overexpress miR-146a was confirmed by qPCR in HTM primary cells as described in the Methods section. Cells transduced with Ad-CAG-miR-146a showed a significant increase in expression (303-fold; $P = 0.0001$; $n = 3$) compared with controls.

Because adenoviral vectors are not the best option for gene therapy due to their relatively high immunogenicity, we tested an scAAV type 2 vector[45] with miR-146a driven by the CAG promoter as well as a control scAAV type 2 expressing GFP under the same promoter. Injection of these vectors at up to 10^{11} pfu in the anterior chamber of living rats did not result in any measurable effect in IOP. Expression of GFP was limited to a very small number of cells in the TM (data not shown); therefore, we generated lentiviral vectors expressing miR-146a under the CAG promoter. The first preparation of lentiviral vector yielded 5.6×10^8 pfu/mL. Given the relatively low titer, we injected 25 µL in the anterior chamber of three Brown Norway rats. Injections of such high volume are likely to result in loss of viral particles, which will exit the anterior chamber due to high pressure and stretching of the TM. It is therefore difficult to evaluate the level of transduction of TM cells in these conditions. However, as shown in Figure 4, injected eyes showed a clear trend toward a decrease in IOP that lasted more than 4 months. The difference in IOP between the injected and the contralateral (non-injected) control eyes decreased over time with an average difference of 2.61 ± 1.43 mmHg (Fig. 4). Expression of Lenti-CAG-miR-146a was confirmed in HTM-transfected cells (12,359 ± 2002 fold; $P = 3.76E\text{-}08$).

A second preparation of the same lentiviral vector yielded a titer of 1×10^9 pfu/mL. With this preparation, we were able to inject six eyes with a total volume of 15 µL per eye. The effects on IOP of these injections were of higher magnitude compared with the previous set of injections and were sustained in all animals for 6 months. In five out the six animals, the effects

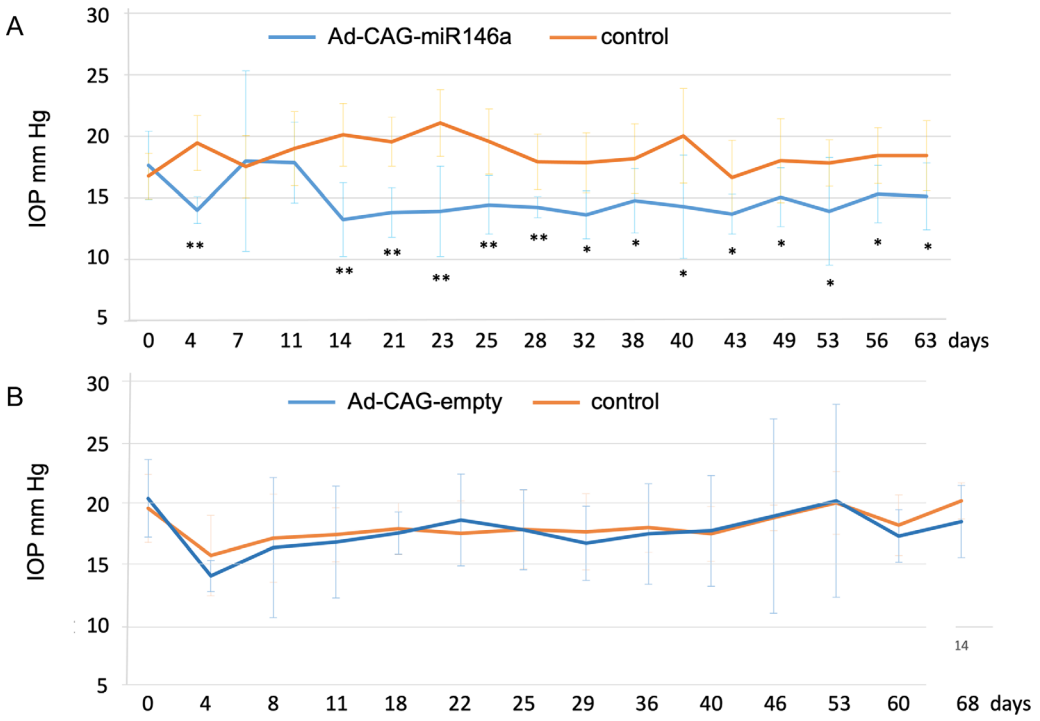

Figure 3. Mean IOP of rat eyes transduced with (**A**) Ad-CAG-miR-146a ($n = 10$) or (**B**) Ad-CAG-empty ($n = 6$). Bars represent mean ± SD. The statistical significance in mean IOP between miR-146a treated and control eyes was calculated using paired *t*-tests at each time point; $^{*}P < 0.05$ and $^{**}P < 0.01$.

were sustained for more than 8 months. There was an average difference of 4.45 ± 2.93 mmHg (Fig. 5).

Effects of Viral Delivery of miR-146a on Visual Function and Morphology

To evaluate whether treatment with Lenti-CAG-miR-146a had any potential adverse effect on eye function, we analyzed visual acuity by involuntary image tracking (optokinetic reflex) using an OptoMotry system at 1.5 and 7 months after injection. The results showed no significant difference in visual acuity between treated and control eyes (Fig. 6). Visual inspections of the eyes did not reveal any obvious abnormalities, such as opacity or corneal edema, at any time during the experiment. Slit-lamp and ophthalmoscope examinations conducted by a certified ophthalmologist at 6 and 7 months revealed no visible abnormalities or signs of inflammation associated with lentivirus delivery of miR-146a. The conjunctiva, cornea, iris, and fundus appearance were scrutinized. No cells or flare were seen in the anterior segment, and no other ocular abnormalities were noted.

Expression of miR-146a and selected inflammatory markers was also evaluated postmortem by qPCR. Tumor necrosis factor alpha (TNFα), cluster of differentation 68 (CD68), interleukin-1 beta (IL-1β), and miR-146a were analyzed in the anterior chamber of three animals. miR-146a was significantly upregulated (4.28 ± 1.97 fold; $P = 0.001$) in the eyes injected with Lenti-CAG-miR-146a 9 months after the injection. Expression of inflammatory markers was not significantly different between eyes injected with Lenti-CAG-miR-146a and the control eyes that were not injected (Fig. 7). Analyses of semi-thin sections of the angle from three rat eyes injected with Lenti-CAG-miR-146a and three non-treated contralateral controls showed no apparent abnormalities or signs of inflammation associated with Lenti-CAG-miR-146a injection and no evident differences with the control eyes (Fig. 8).

Discussion

Previous experiments in our laboratory using HTM cells suggested a potential role of miR-146a as a modulator of IOP due to its ability to alter the expression of genes that could affect outflow homeostasis and because miR-146a itself was upregulated under CMS.[29,30] In this study we showed that miR-146a alters

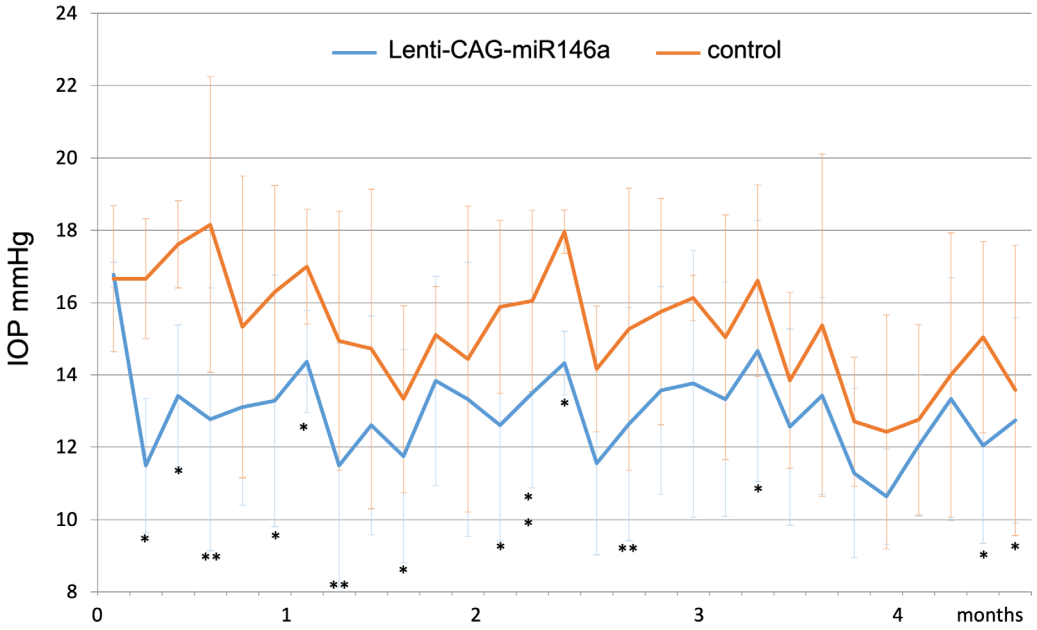

Figure 4. Mean IOP of rat eyes transduced with Lenti-CAG-miR-146a at 5.8×10^8 pfu/mL compared with non-treated controls ($n = 3$). Bars represent mean ± SD. The statistical significance in mean IOP between miR-146a–treated and control eyes was calculated using paired *t*-tests at each time point; $^{*}P < 0.05$ and $^{**}P < 0.01$.

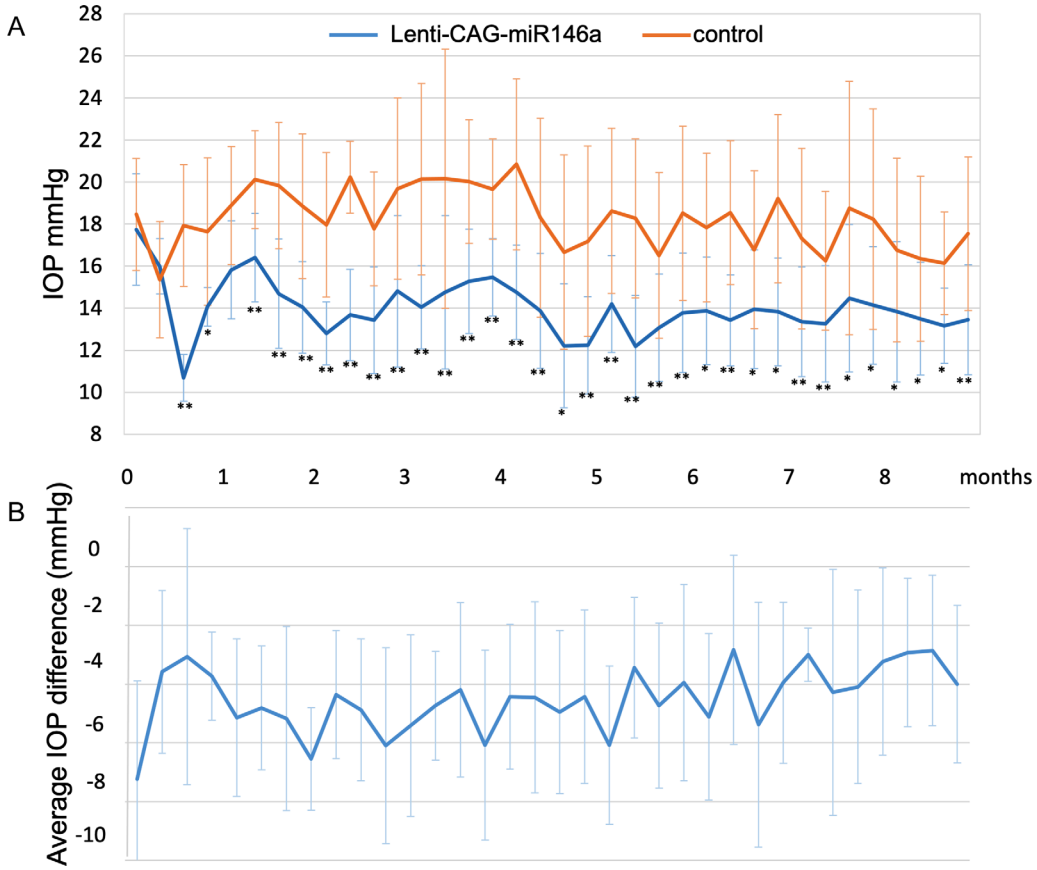

Figure 5. (**A**) Average IOP and (**B**) average IOP difference in rat eyes transduced with Lenti-CAG-miR-146a at 1.0×10^9 pfu/mL compared with non-treated controls eyes ($n = 6$). Bars represent mean ± SD. The statistical significance in mean IOP between miR-146a–treated and control eyes was calculated using paired *t*-tests at each time point; $^{*}P < 0.05$ and $^{**}P < 0.01$.

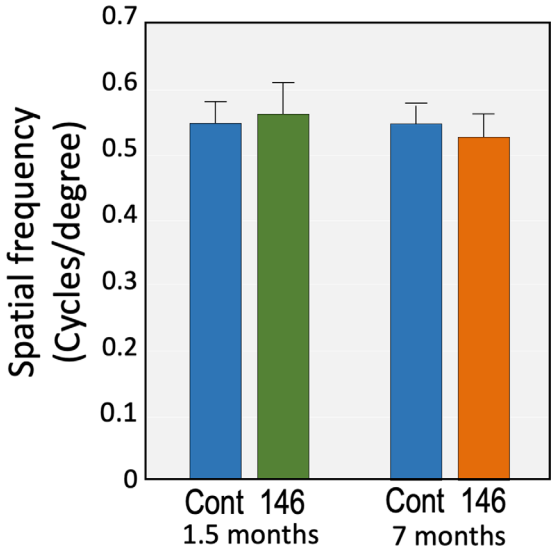

Figure 6. Visual acuity of rat eyes injected with miR-146a. Spatial frequency was used as a measure of visual function and evaluated by OKT at two time points (1.5 and 7 months) after injection. No significant differences were observed between Lenti-CAG-miR-146a–injected eyes (146) and un-injected control eyes (Cont). Bars represent mean ± SD.

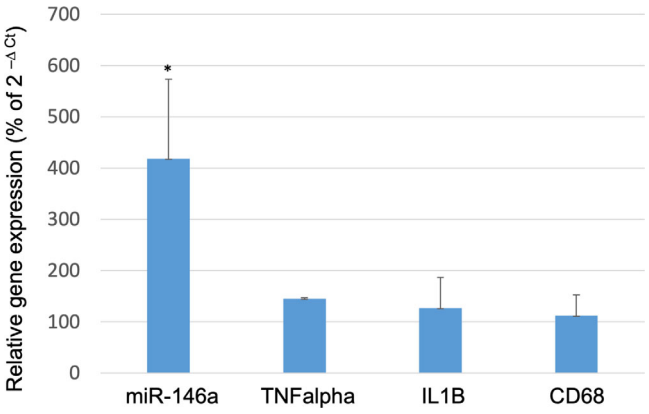

Figure 7. Expression of inflammatory genes in the anterior chamber of rat eyes transduced with miR-146a. Inflammatory markers (TNFα, IL-1β, and CD68), as well as miR-146a, were analyzed by qPCR 9 months after rat eyes were transduced with Lenti-CAG-miR-146a. Gene expression is represented as a percentage of expression in untreated control eyes (100%). Bars represent mean ± SD. Statistical significance was calculated using unpaired *t*-tests; $^{*}P < 0.05$.

the expression of these genes at basal level and/or under CMS. To gain knowledge of its effects in vivo we injected miR-146a in the anterior chamber of rat eyes. Our results showed that the administration of adenoviral and lentiviral miR-146a to the anterior chamber of normotensive rats significantly reduces IOP. Although the results from the administration of 25 µL per eye of Lenti-CAG-miR-146a at 5.6×10^8 pfu/mL could be interpreted as just a trend given the small number of animals, administration of 15 µL at 1.0×10^9 pfu/mL in six rats provided a robust and sustained decrease of IOP for more than 8 months in most animals. These results suggest that optimizing the volume, titer, and method of administration might improve the intensity and duration of the effects of miR-146 on IOP.

Our initial hypothesis was that miR-146 could act as a brake in the production of inflammatory cytokines. Given that production of some inflammatory cytokines by TM cells in response to mechanical stress had been shown to increase aqueous humor outflow facility,[46] we hypothesized that the induction of miR-146a could elevate IOP. Previous experiments using a different construct of miR-146 (influenza-associated virus–CMV promoter–mature miRNA) produced a transient increase in IOP in rats (Luna C. *IOVS*. 2014; 55:ARVO E-Abstract 4516). However, levels and duration of transgene expression with this vector were substantially lower than those achieved with either Ad-CAG-miR-146a or Lenti-CAG-miR-146a.

Although the reasons for the decrease in intraocular pressure induced by miR-146a (adenovirus and lentivirus) in rats have not been elucidated, there are several possible mechanisms, alone or in combination, that could contribute to this effect. miR-146a has been shown to play significant roles as a negative regulator of the inflammatory response and fibrosis. Also, miR-146a has been shown to decrease the inflammatory response in mice and humans mainly by attenuating nuclear factor kappa B (NF-κB) signaling through its targets TRAF6 and IRAK1, affecting downstream factors such as IL-1β, IL-6, IL-8, and TNFα.[47–49] NF-κB regulates the expression of a vast number of genes that could potentially affect outflow. Specifically, it plays a key role in the regulation of autotaxin, a major producer of lisophosphatidic acid (LPA).[50,51] Both, autotaxin and LPA are known to be increased in the aqueous humor of open-angle glaucoma patients. Inhibition of autotaxin has been shown to increase aqueous outflow ex vivo.[52] Therefore, the effect of miR-146a on NF-κB could potentially affect outflow facility through modulation of LPA and autotaxin levels.

miR-146a is also a negative regSulator of transforming growth factor- beta (TGF-β) by targeting Smad4 in several cell types, and in vivo it attenuated the fibrotic markers induced by TGF-β.[53,54] Although the mechanisms that contribute to high IOP in glaucoma are complex, TGF-β1 and TGF-β2 are potent profibrotic factors that have been shown to be directly implicated in the pathogenesis of IOP[55–57] and to be elevated in the aqueous humor of glaucoma patients.[58] Plasminogen activator inhibitor 1 (*PAI1*) is another gene downregulated by miR-146 in HTM cells.[29] *PAI1*

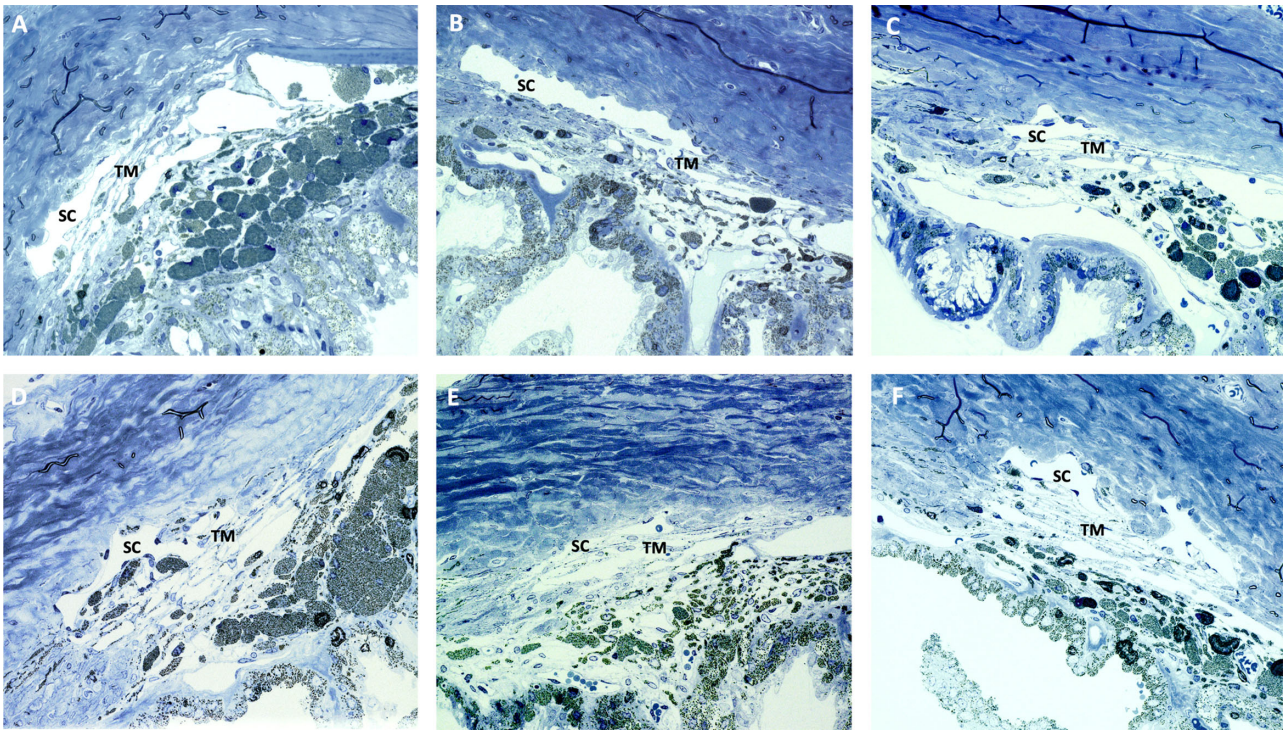

Figure 8. Semi-thin sections of rat eyes angle transduced with Lenti-CAG-miR-146a or contralateral control eyes 9 months after injection. (**A**–**C**) Representative images of Lenti-CAG-miR-146a transduced eyes. (**D**–**F**) Representative images of contralateral eyes ($n = 3$). SC, Schlemm's canal; TM, trabecular meshwork.

is the main inhibitor of the extracellular proteinases, tissue and urokinase plasminogen activators (tPA and uPA). An increase in *PAI1* could lead to extracellular matrix deposition in the aqueous humor and trabecular meshwork. Glucocorticoid treatment of HTM cells increases *PAI1*. Blocking this increase could be partially responsible for lowering IOP in vivo using a steroid agonist.[59] miR-146 could act as a mechanosensor in certain cell types. For example, in lung epithelial cells, miR-146a was upregulated by oscillatory pressure and/or TNFα. miR-146a can regulate mechanical induced inflammation[60] and in human chondrocyte was involved in apoptosis in response to mechanical injury.[61] Our experiments involving analyses of gene expression changes induced by CMS had intrinsic levels of variability among different experiments due to the nature of the experimental model, as observed by the differences in gene expression induced by CMS in cells transfected with scrambled mimic compared to those transfected with scrambled inhibitor. However, the results consistently demonstrated the ability of miR-146a to alter the response of certain genes induced by CMS; among these are *PAI1* and several cytokines. These results, together with the previously reported observation that miR-146a is induced by CMS in HTM cells,[29,30] might contribute to modulating some of the effects of CMS in the TM.

Finally, miR-146a has been shown to target Rho kinase 1 (ROCK1) in several cell types.[62,63] Given the known IOP-lowering effects of pharmacological inhibition of ROCK1,[64] targeting this protein could also potentially contribute to the observed effects of miR-146a in living rat eyes. Therefore, with the pleiotropic effects of miR-146, multiple mechanisms could be involved in the observed effects on IOP in living rat eyes. Specific studies aimed at determining such mechanisms are necessary to understand the relative roles of different genes and pathways regulated by miR-146a in IOP. Eyes transduced with miR-146a showed no signs of inflammation. This is possibly due to its antiinflammatory effect but could also be because miRNAs have shown low toxicity and immunogenicity when compared with DNA gene therapy or protein-based drug molecules.[23]

The current study has some important limitations. These include the small number of animals and lack of a lentivirus control. However, control lentiviral vectors (HIV- or feline immunodeficiency virus–based) have been tested previously in rats and other species and have consistently shown no significant effects on IOP. [4,15,17,19,65] Specifically, the lentivirus system with the CAG promoter was tested in rats by Tan et al.,[15] and the controls did not show any significant effect on IOP, similar to what we observed in

our results for the adenoviral vector. Therefore, we believe that the results strongly suggest that administration of a lentivirus expressing miR-146a to the cells of the anterior chamber of living rats can decrease IOP without obvious adverse effects for more than 8 months. miR-146a appears to be a promising candidate for developing an effective gene therapy for sustained control of IOP in glaucoma patients.

Acknowledgments

We thank Ying Hao at the Duke Eye Center Morphology facility for her invaluable collaboration preparing the semi-thin sections for morphological analysis.

Supported by grants from the National Eye Institute, National Institutes of Health (EY029400 and EY05722) and by The Glaucoma Foundation.

Disclosure: **C. Luna,** (P); **M. Parker,** None; **P. Challa,** None; **P. Gonzalez,** (P)

References

1. Peters D, Bengtsson B, Heigl A. Lifetime risk of blindness in open-angle glaucoma. *Am J Ophthalmol*. 2013;156:724–730.
2. Lee JH, Wang JH, Chen J, Li F, Edwards TL, Hewitt AW, Liu GS. Gene therapy for visual loss: Opportunities and concerns. *Prog Retin Eye Res*. 2019;68:31–53.
3. Moreno-Montañés J, Sádaba B, Ruz V, et al. Phase I clinical trial of SYL040012, a small interfering RNA targeting β-adrenergic receptor 2, for lowering intraocular pressure. *Mol Ther*. 2014;22:226–232.
4. Barraza RA, Rasmussen CA, Loewen N, et al. Prolonged transgene expression with lentiviral vectors in the aqueous humor outflow pathway of nonhuman primates. *Hum Gene Ther*. 2009;20:191–200.
5. Spiga MG, Borrás T. Development of a gene therapy virus with a glucocorticoid-inducible MMP1 for the treatment of steroid glaucoma. *Invest Ophthalmol Vis Sci*. 2010;51:3029–3041.
6. Barraza RA, McLaren JW, Poeschla EM. Prostaglandin pathway gene therapy for sustained reduction of intraocular pressure. *Mol Ther*. 2010;18:491–501.
7. Gerometta R, Spiga MG, Borrás T, Candia OA. Treatment of sheep steroid-induced ocular hypertension with a glucocorticoid-inducible MMP1 gene therapy virus. *Invest Ophthalmol Vis Sci*. 2010;51:3042–3048.
8. Borrás T. Gene therapy strategies in glaucoma and application for steroid-induced hypertension. *Saudi J Ophthalmol*. 2011;25:353–362.
9. Kumar S, Shah S, Tang HM, Smith M, Borrás T, Danias J. Tissue plasminogen activator in trabecular meshwork attenuates steroid induced outflow resistance in mice. *PLoS One*. 2013;8:e72447.
10. Borrás T, Buie LK, Spiga MG. Inducible scAAV2.GRE.MMP1 lowers IOP long-term in a large animal model for steroid-induced glaucoma gene therapy. *Gene Ther*. 2016;23:438–449.
11. Borrás T. The pathway from genes to gene therapy in glaucoma: a review of possibilities for using genes as glaucoma drugs. *Asia Pac J Ophthalmol (Phila)*. 2017;6:80–93.
12. Dillinger AE, Guter M, Froemel F, et al. Intracameral delivery of layer-by-layer coated siRNA nanoparticles for glaucoma therapy. *Small*. 2018;14:e1803239.
13. O'Callaghan J, Cassidy PS, Humphries P. Open-angle glaucoma: therapeutically targeting the extracellular matrix of the conventional outflow pathway. *Expert Opin Ther Targets*. 2017;21:1037–1050.
14. O'Callaghan J, Crosbie DE, Cassidy PS, et al. Therapeutic potential of AAV-mediated MMP-3 secretion from corneal endothelium in treating glaucoma. *Hum Mol Genet*. 2017;26:1230–1246.
15. Tan J, Liu G, Zhu X, et al. Lentiviral vector-mediated expression of exoenzyme C3 transferase lowers intraocular pressure in monkeys. *Mol Ther*. 2019;27:1327–1338.
16. Tan J, Fan N, Wang N, et al. Effects of lentivirus-mediated C3 expression on trabecular meshwork cells and intraocular pressure. *Invest Ophthalmol Vis Sci*. 2018;59:4937–4944.
17. Lee ES, Rasmussen CA, Filla MS, et al. Prospects for lentiviral vector mediated prostaglandin F synthase gene delivery in monkey eyes in vivo. *Curr Eye Res*. 2014;39:859–870.
18. Slauson SR, Peters DM, Schwinn MK, Kaufman PL, Gabelt BT, Brandt CR. Viral vector effects on exoenzyme C3 transferase-mediated actin disruption and on outflow facility. *Invest Ophthalmol Vis Sci*. 2015;56:2431–2438.
19. Xiang Y, Li B, Wang JM, et al. Gene transfer to human trabecular meshwork cells in vitro and ex vivo using HIV-based lentivirus. *Int J Ophthalmol*. 2014;7:924–929.
20. Wu J, Bell OH, Copland DA, et al. Gene therapy for glaucoma by ciliary body aquaporin

1 disruption using CRISPR-Cas9. *Mol Ther*. 2020;28(3):820–829.
21. Komáromy AM. CRISPR-Cas9 Disruption of aquaporin 1: an alternative to glaucoma eye drop therapy? *Mol Ther*. 2020;28(3):706–708.
22. Laffont B, Rayner KJ. MicroRNAs in the pathobiology and therapy of atherosclerosis. *Can J Cardiol*. 2017;33:313–324.
23. Chen Y, Gao DY, Huang L. In vivo delivery of miRNAs for cancer therapy: challenges and strategies. *Adv Drug Deliv Rev*. 2015;81:128–141.
24. Bhatt K, Lanting LL, Jia Y, et al. Anti-inflammatory role of microRNA-146a in the pathogenesis of diabetic nephropathy. *J Am Soc Nephrol*. 2016;27:2277–2288.
25. Cowan C, Muraleedharan CK, 3rd O'Donnell JJ, et al. MicroRNA-146 inhibits thrombin-induced NF-κB activation and subsequent inflammatory responses in human retinal endothelial cells. *Invest Ophthalmol Vis Sci.* 2014;55:4944–4951.
26. Chen S, Feng B, Thomas AA, Chakrabarti S. miR-146a regulates glucose induced upregulation of inflammatory cytokines extracellular matrix proteins in the retina and kidney in diabetes. *PLoS One*. 2017;12:e0173918.
27. Feng B, Chen S, Gordon AD, Chakrabarti S. miR-146a mediates inflammatory changes and fibrosis in the heart in diabetes. *J Mol Cell Cardiol*. 2017;105:70–76.
28. Javidan A, Jiang W, Okuyama M, et al. miR-146a deficiency accelerates hepatic inflammation without influencing diet-induced obesity in mice. *Sci Rep*. 2019;9:12626.
29. Li G, Luna C, Qiu J, Epstein DL, Gonzalez P. Modulation of inflammatory markers by miR-146a during replicative senescence in trabecular meshwork cells. *Invest Ophthalmol Vis Sci*. 2010;51:2976–2985.
30. Luna C, Li G, Qiu J, Epstein DL, Gonzalez P. MicroRNA-24 regulates the processing of latent TGFβ1 during cyclic mechanical stress in human trabecular meshwork cells through direct targeting of FURIN. *J Cell Physiol*. 2011;226:1407–1414.
31. Davies PF, Tripathi SC. Mechanical stress mechanisms and the cell. An endothelial paradigm. *Circ Res*. 1993;72:239–245.
32. Wang JH, Thampatty BP. An introductory review of cell mechanobiology. *Biomech Model Mechanobiol*. 2006;5:1–16.
33. Liton PB, Gonzalez P. Stress response of the trabecular meshwork. *J Glaucoma*. 2008;7:378–385.
34. Vittal V, Rose A, Gregory KE, Kelley MJ, Acott TS. Changes in gene expression by trabecular meshwork cells in response to mechanical stretching. *Invest Ophthalmol Vis Sci.* 2005;46:2857–2868.
35. Gonzalez P, Epstein DL, Borras T. Genes upregulated in the human trabecular meshwork in response to elevated intraocular pressure. *Invest Ophthalmol Vis Sci.* 2000;41:352–361.
36. Tumminia SJ, Mitton KP, Arora J, Zelenka P, Epstein DL, Russell P. Mechanical stretch alters the actin cytoskeletal network and signal transduction in human trabecular meshwork cells. *Invest Ophthalmol Vis Sci*. 1998;39:1361–1371.
37. Vittitow J, Borras T. Genes expressed in the human trabecular meshwork during pressure-induced homeostatic response. *J Cell Physiol.* 2004;201:126–137.
38. Keller KE, Bhattacharya SK, Borrás T, et al. Consensus recommendations for trabecular meshwork cell isolation, characterization and culture. *Exp Eye Res*. 2018;171:164–173.
39. Untergasser A, Cutcutache I, Koressaar T, et al. Primer3–new capabilities and interfaces. *Nucleic Acids Res*. 2012;40:e115.
40. Matsuda T, Cepko CL. Electroporation and RNA interference in the rodent retina in vivo and in vitro. *Proc Natl Acad Sci USA*. 2004;101:16–22.
41. Taganov KD, Boldin MP, Chang KJ, Baltimore D. NF-kappaB-dependent induction of microRNA miR-146, an inhibitor targeted to signaling proteins of innate immune responses. *Proc Natl Acad Sci USA*. 2006;103:12481–12486.
42. Pekrun K, De Alencastro G, Luo QJ, et al. Using a barcoded AAV capsid library to select for clinically relevant gene therapy vectors. *JCI Insight.* 2019;4:e131610.
43. Labidi-Galy SI, Clauss A, Ng V, et al. Elafin drives poor outcome in high-grade serous ovarian cancers and basal-like breast tumors. *Oncogene*. 2015;34:373–383.
44. Douglas RM, Alam NM, Silver BD, McGill TJ, Tschetter WW, Prusky GT. Independent visual threshold measurements in the two eyes of freely moving rats and mice using a virtual-reality optokinetic system. *Vis Neurosci*. 2005;22:677–684.
45. Borrás T, Xue W, Choi VW, et al. Mechanisms of AAV transduction in glaucoma-associated human trabecular meshwork cells. *J Gene Med*. 2006;8:589–602.
46. Liton PB, Luna C, Bodman M, Hong A, Epstein DL, Gonzalez P. Induction of IL-6 expression by mechanical stress in the trabecular meshwork. *Biochem Biophys Res Commun*. 2005;337:1229–1236.

47. Saba R, Sorensen DL, Booth SA. MicroRNA-146a: a dominant, negative regulator of the innate immune response. *Front Immunol*. 2014;5: 578.
48. Zheng CZ, Shu YB, Luo YL, Luo J. The role of miR-146a in modulating TRAF6-induced inflammation during lupus nephritis. *Eur Rev Med Pharmacol Sci*. 2017;21:1041–1048.
49. Wei J, Wang J, Zhou Y, Yan S, Li K, Lin H. MicroRNA-146a contributes to SCI recovery via regulating *TRAF6* and *IRAK1* expression. *Biomed Res Int*. 2016;2016:4013487.
50. Murph MM. MicroRNA regulation of the autotaxin-lysophosphatidic acid signaling axis. *Cancers (Basel)*. 2019;11:1369.
51. Wu JM, Xu Y, Skill NJ, et al. Autotaxin expression and its connection with the TNF-alpha-NF-kappaB axis in human hepatocellular carcinoma. *Mol Cancer*. 2010;9:71.
52. Ho LTY, Osterwald A, Ruf I, et al. Role of the autotaxin-lysophosphatidic acid axis in glaucoma, aqueous humor drainage and fibrogenic activity. *Biochim Biophys Acta Mol Basis Dis*. 2020;1866:165560.
53. Sun Y, Li Y, Wang H, et al. miR-146a-5p acts as a negative regulator of TGF-β signaling in skeletal muscle after acute contusion. *Acta Biochim Biophys Sin (Shanghai)*. 2017;49:628–634.
54. Min SK, Jung SY, Kang HK, Jo SB, Kim MJ, Min BM. MicroRNA-146a-5p limits elevated TGF-β signal during cell senescence. *Mol Ther Nucleic Acids*. 2017;7:335–338.
55. Battacharya SK, Gabelt BT, Ruiz J, Picciani R, Kaufman PL. Cochlin expression in anterior segment organ culture models after TGFbeta2 treatment. *Invest Ophthalmol Vis Sci.* 2009;50:551–559.
56. Shepard AR, Millar JC, Pang IH, Jacobson N, Wang WH, Clark AF. Adenoviral gene transfer of active human transforming growth factor-β2 elevates intraocular pressure and reduces outflow facility in rodent eyes. *Invest Ophthalmol Vis Sci.* 2010;51:2067–2076.
57. Robertson JV, Golesic E, Gauldie J, West-Mays JA. Ocular gene transfer of active TGF-β induces changes in anterior segment morphology and elevated IOP in rats. *Invest Ophthalmol Vis Sci*. 2010;51:308–318.
58. Prendes MA, Harris A, Wirostko BM, Gerber AL, Siesky B. The role of transforming growth factor β in glaucoma and the therapeutic implications. *Br J Ophthalmol.* 2013;97:680–686.
59. Robin AL, Suan EP, Sjaarda RN, et al. Reduction of intraocular pressure with anecortave acetate in eyes with ocular steroid injection-related glaucoma. *Arch Ophthalmol*. 2009;127:173–178.
60. Huang Y, Crawford M, Higuita-Castro N, Nana-Sinkam P, Ghadiali SN. miR-146a regulates mechanotransduction and pressure-induced inflammation in small airway epithelium. *FASEB J*. 2012;26:3351–3364.
61. Jin L, Zhao J, Jing W, et al. Role of miR-146a in human chondrocyte apoptosis in response to mechanical pressure injury in vitro. *Int J Mol Med.* 2014;34:451–463.
62. Xu B, Huang Y, Niu X, et al. Hsa-miR-146a-5p modulates androgen-independent prostate cancer cells apoptosis by targeting ROCK1. *Prostate*. 2015;75:1896–1903.
63. Wang G, Huang Y, Wang LL, et al. MicroRNA-146a suppresses ROCK1 allowing hyperphosphorylation of tau in Alzheimer's disease. *Sci Rep*. 2016;6:26697.
64. Honjo M, Tanihara H. Impact of the clinical use of ROCK inhibitor on the pathogenesis and treatment of glaucoma. *Jpn J Ophthalmol*. 2018;62:109–126.
65. Khare PD, Loewen N, Teo W, et al. Durable, safe, multi-gene lentiviral vector expression in feline trabecular meshwork. *Mol Ther.* 2008;16:97–106.